The 9th European Congress on Computational Methods in Applied Sciences and Engineering
ECCOMAS Congress 2024
3–7 June 2024, Lisboa, Portugal

FUEL BURN EFFICIENCY POTENTIAL OF LOAD ALLEVIATION AND WING PLANFORM OPTIMIZATION IN CONCEPTUAL OVERALL AIRCRAFT DESIGN

Markus D. Krengel[1]

[1] German Aerospace Center (DLR e.V.)
Institute of Aerodynamics and Flow Technology
Lilienthalplatz 7, 38108 Braunschweig, Germany
e-mail: markus.krengel@dlr.de, www.dlr.de

Key words: Conceptual Aircraft Design, Load Alleviation, Flexible Wing, Multidisciplinary Optimization

Summary. This study shows the integration of the overall aircraft design with a concurrent wing planform optimization for long-range aircraft. The focus is on wing design and active load control with trailing edge flaps. A physics-based framework for structural wing design with simplified aeroelastic load cases is the computational backbone of the research. The goal is to explore the potential of load alleviation while optimizing a conventional cantilever aircraft configuration with a surrogate model based approach. It is shown that load alleviation significantly reduces the wing mass, and has an effect on the empennage. In comparing optimized aircraft designs with and without load alleviation, the fuel burn benefit of load alleviation is between 1.6% and 19.5%, with 11.6% as the most realistic estimate. This includes a 4% improvement from active load alleviation and 7.6% from the wing planform optimization. Simplified constraints like maximum wingspan and minimum roll control authority are investigated. Implicit conditions such as constant wing loading and static margin are included to ensure comparability across the designs.

1 INTRODUCTION

Comparing the increase in available seat kilometers (ASK) [1] with the global carbon dioxide (CO2) emissions from aviation [2] shows rising yet decoupled trends. By 2019, the ASK had expanded nearly 300-fold since the 1950s, while the CO2 emissions had increased less than 20-fold. This suggests an enhanced efficiency in air travel, through better aircraft utilization and primarily technological advances. Fuel cost savings and recent environmental concerns have propelled this progress. The European Union (EU) targets a 75% reduction in CO2 emissions by 2050 compared to the 2000 levels, as outlined in the European Green Deal [3] and the aviation-specific Flightpath 2050 [4, 5]. The German Aerospace Center (DLR) aligns with the Green Deal with goals for 2050: reducing fuel consumption by 25%, achieving 50% more energy-efficient aircraft, and decreasing climate impact by 30% through optimized flight paths [6]. However, even in the best-case scenario, these measures alone will not fulfill the EU's goal of net-zero emissions; an additional 17% reduction must be compensated elsewhere. In the USA, also NASA's ambitious objectives for the N+3 aircraft generation, anticipated for the post-2035 aircraft, include a 60-80% decrease in fuel consumption [7–9].

There is a clear mismatch between the current evolutionary trend in aviation and future efficiency targets. Main improvements have been primarily related to engine enhancements. However, additional gains are becoming challenging due to limits in feasible bypass ratios [10]. This necessitates the exploration of additional technological advancements. The IATA Aircraft Technology Net Zero Roadmap [11] proposes new technologies, such as configuration-independent active load alleviation. Many future aircraft designs incorporate high aspect ratio wings, where active load alleviation is relevant [12–18]. Given potential flight altitude restrictions due to climate impact, enhancing load alleviation becomes even more significant at lower altitudes with higher gust loads [19]. Active control technologies, described already in the 1960s, were demonstrated by Noll et al. for maneuver and gust load alleviation in 1993 [20]. Handojo et al. showed a significant 26.5% reduction in wing mass for long-range aircraft with these techniques [21]. Binder et al. [22] showed that maneuver load alleviation already accounts for 72% of potential load reductions, that all mechanism (maneuver and gust load as well as structural tailoring) combined can achieve. Studies like those by Thel et al. have focused on the passive structural tailoring by optimizing the wing bending-torsion coupling without altering the wing design [23]. Also a wing planform optimization is of interest for overall efficiency gains: Liem et al. [24] conducted a multi-point block fuel optimization of a long-range aircraft, resulting in a higher aspect ratio and a 6.6% reduction in fuel burn. Ricci et al. [25] performed a simplified aspect ratio study of a wing, identifying an optimal aspect ratio of 15 correlated to a block fuel saving of 9.9% for a short and medium-range aircraft.

Combining load alleviation with wing shape optimization is a natural progression in this specific research area. Wunderlich et al. [26] presented an approach including the DLR TAU software (RANS code) for a long-range aircraft, achieving a combined block fuel reduction of 12.9% compared to a baseline configuration and 4.3% reduction in combined fuel burn between the Optima with and without load alleviation. Similarly, Xu and Kroo [27] evaluated a short-range aircraft with a flexible wing, based on conceptual methods. They reported a fuel burn reduction of 11 % for a turbulent wing with active load alleviation.

Early integration of load alleviation in the design phase is important since it is affecting wing shape and performance. At later design stages the wing planform and outer shape are largely fixed. However, already this early stage integration requires physics-based models of aerodynamics, structural dynamics, and flight control while maintaining a manageable model fidelity for extensive computational studies.

Active load alleviation remains particularly relevant for long-range aircraft, as highlighted by the DLR strategy [6]. It is crucial for reducing structural weight. For assessment clarity, it is beneficial to distinguish load alleviation technology from future aircraft design effects. This paper focuses on wing optimization with active load alleviation, retaining the traditional tube and wing configuration, but the insights may also apply to future designs. The work presented here is based on previous investigations [28, 29].

2 METHODOLOGY

The framework for conceptual aircraft design used here is based on the overall aircraft design environment OpenAD [30]. ASWING from Drela [31, 32] is included as a physics-engine, modeling the flexible aircraft within an overall design framework. Figure 1 shows the general structure and data flow of the framework.

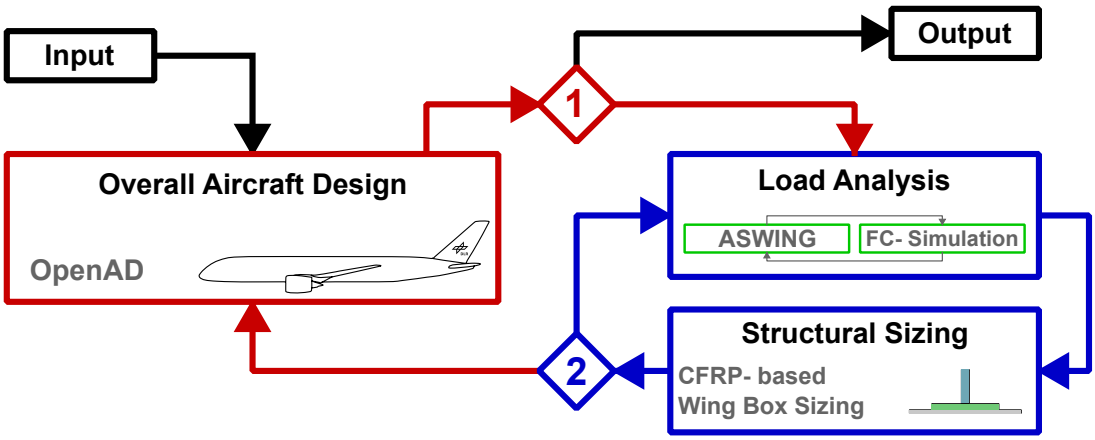

Figure 1: Overview of the entire process flow for dynamic aeroelastic wing sizing.

All data flows between the modules are based on the CPACS file scheme [33]. Initial inputs include the Top Level Aircraft Requirements, constraints, and calibration factors. The process returns a converged aircraft design, including a wing description with values from the physics-based sizing. The framework features two cascading loops. The outer loop (**1**) updates the overall aircraft design with the wing mass and the aerodynamic efficiency from the physics-based wing sizing in loop 2, with a maximum take-off mass convergence criteria by Cauchy's classic definition [34]. The inner loop (**2**) iteratively computes the wing stiffness and mass distribution, factoring in load cases simulated within ASWING including the control simulation. The sizing of the secondary wing structures is based on handbook methods [35]. The framework adjusts the aircraft components like landing gears and tail planes according to the handbook methods implemented in OpenAD [30], while maintaining stability margins and wing loading. In addition to ASWING, the wave drag is locally approximated to improve the performance calculation via the Korn equation, as illustrated in Mason [36]. Employing the transformation rules for swept wings, as described in Obert [37], the wave drag can be expressed in the direction of the incoming undisturbed flow. As the shock position is typically situated near 50 % of the chord length, the corresponding sweep of the 50 % line is utilized here. Figure 2 illustrates a typical ASWING model representation of an exemplary long-range aircraft.

A simple approach for gust load alleviation involves a control of the lift coefficient of the aircraft based on the cruise level flight. To ensure a working controller with constant gains the short-term oscillation of the aircraft is adjusted to constant behavior for good handling qualities via two feedback loops. The gust load controller used here is depicted in Figure 3. Krengel and Hepperle [28] demonstrated the effectiveness of this simplified approach in this context.

All flaps are modeled as plain flaps, with their local impact estimated via Glauert's formula [38]. The maximum movement rate for Ailerons and Elevator is set to 35°/sec and the acceleration limit of 400°/sec^2. For more details see Krengel and Hepperle [28, 29].

2.1 Considered load cases and load alleviation

At conceptual aircraft design level, due to the limited detail of the models, it is necessary and, considering the computational time, also desirable to incorporate only flight loads with the most significant impact on the global wing structure. The loads here are therefore simplified

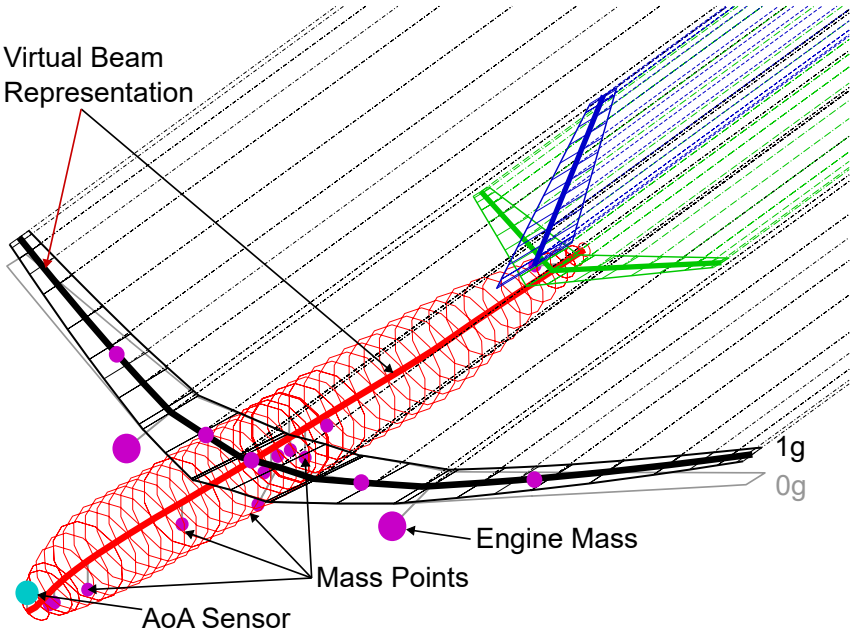

Figure 2: ASWING representation of an exemplary long range aircraft.

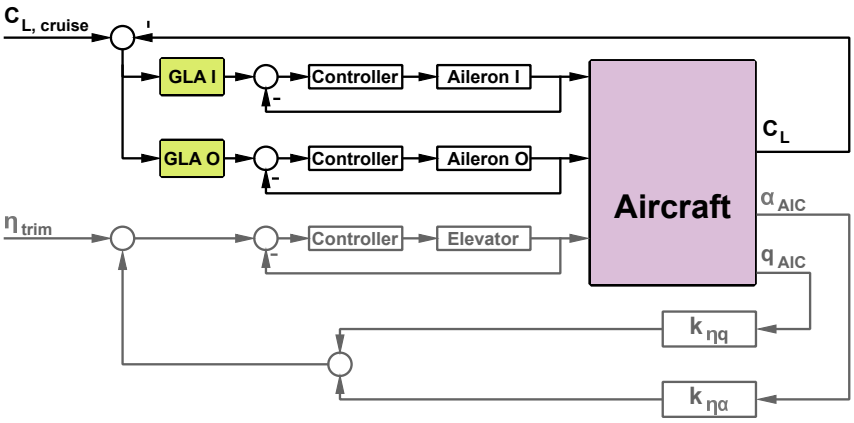

Figure 3: Controller feedback loops for pitch damping and GLA.

and primarily based on the assumption of four flight points presented in Table 2.1.

The design cruise flight point, denoted as C and a slightly higher dive Mach number (denoted as D) are examined. Additionally, a climb flight point (m) and a basic high-lift case (F) are evaluated. The climb point features a 3° flight path angle with a moderate speed. The high-lift case involves the aircraft with extended inboard and outer flaps at angles of 28° and 15°, respectively, trimmed at a lower airspeed of 131 knots near the ground level. Since there is an active local limit for the maximum lift coefficient within the ASWING model, the maneuver load cases are transferred to the ground level at a constant Equivalent Air Speed (EAS).

The focus here is on quasi-steady maneuver loads for pull-up, push-down, and roll cases with a 30° bank angle. Figure 4 illustrates the considered maneuver loads in a v-N diagram.

Table 1: Flight points for the analysis.

	EAS [kts]	Altitude [m]	Flap Setting	Flight Path Angle [°]	Condition
v_C	266	10 668	UP	+0.0	Cruise
v_m	272	5 462	UP	+3.0	Climb
v_D	289	10 668	UP	−3.5	Dive
v_F	131	100	DOWN	+4.0	High Lift

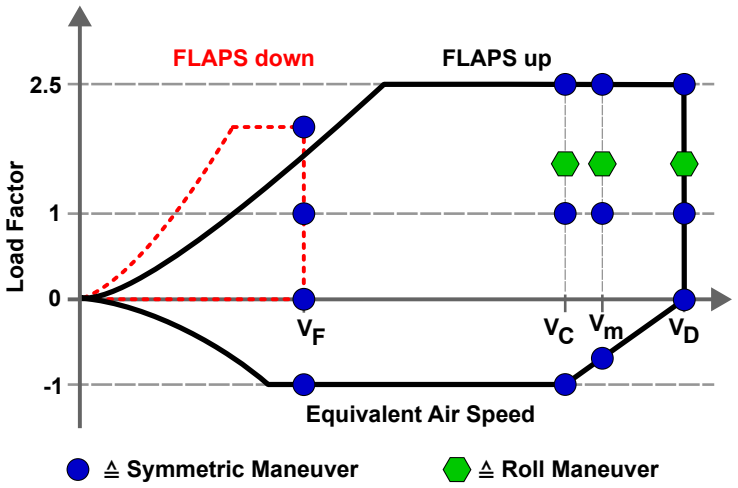

Figure 4: Maneuver load cases for the analysis.

The deflection for maneuver load alleviation (MLA) relates linearly to the equivalent airspeed and the commanded load factor n_z. The maximum deflection occurs at with a load factor of -1.0 (maximum delta to a load factor of 1.0) at the dive velocity. The maximum deflection angles for MLA are: -16° for the inner, 19° for the outer flap, 20° for the inner and 15° for the outer aileron.

The gust load scenarios analyzed here are 1-Cos gusts. Following the CS25 [39] requirements, gusts are modeled for wavelengths of 9, 58, and 107 meters, considering both positive and negative vertical gust velocities. This results in 24 distinct gust load cases.

2.2 Design space, target function and boundary conditions

The design space here is formed in total by nine paramters, which are shown in Figure 5. There are four planform parameter: the aspect ratio AR, the taper ratio TR, the leading edge sweep angle φ_{LE} and the relative kink position η_K. The twist distribution of the wing is defined at three stations: the kink station, the mid station, and the tip station. In-between these stations the distributions are linear. The mid station is defined at a relative span of 60%.

A comprehensive overall metric for the comparison of aircraft configurations is the fuel consumption as it inherently includes all essential disciplinary effects. In practice, many aircraft operated by airlines do not fly the design mission and typically operate at much shorter dis-

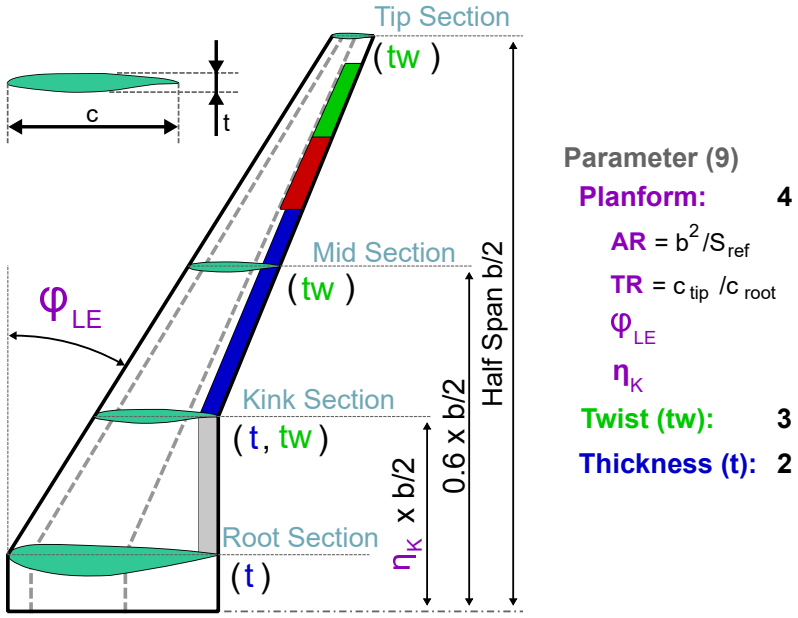

Figure 5: Selected design space for optimization and analysis.

tances with reduced payload capacities. Adler and Martins [40] also showed the benefits of a multi-point target function. Here, in addition to the design mission, the analysis also considers two other relevant study missions. The design transport task for all aircraft designs here is equivalent to that of the reference configuration. The design mission requires transporting 270 passengers (PAX) or 31.05 tons over 6000 nautical miles at an initial cruise Mach number of 0.83. The maximum payload is 34 tons. The mission with the highest relevance here is defined by 75% of the design payload at a range of approximately 4000 NM. In addition, there is a significant number of flights around a range of 2000 NM. This matches many typical distances in the near and far east as for example Dubai to Katar. Since these regions are expected to grow in required available seat kilometer [41], it is possible that some operators might fully load the aircraft to maximum payload for shorter ranges. Together with the design mission a combined specific block fuel is calculated as decribed in detail in Krengel and Hepperle [28]. Later block fuel values will refer to this combination of missions as *block fuel* $BF_{r,c}$.

To avoid unfeasible aircraft designs, particularly within the optimization, where specific constraints must be considered, this thesis assumes relevant but simplified boundary conditions. The following limitations are considered here also for the optimization with the exception of the landing gear constraint as it is far to limiting on the conceptual design level:

- The mission fuel fits within the wing tank volume, termed the *Tank Constraint*;
- the wingspan fits within a 65 m box, referred to as the *Span Constraint*;
- the main landing gear tire diameter fits behind the rear spar (*MLG Constraint*);
- and the effectiveness of the high-speed roll control of the outer aileron is at least 60%, and that of the inner aileron at 80%, compared to the reference aircraft (*Roll Constraint*).

For the global trend study a fully connected feed forward neural network with 15 neurons in six hidden layers is trained, based on the global block fuel as output layer and the nine design parameters as the input layer. Feed forward here means that information is passed only in one direction without recirculation [42]. Neural networks exhibit enhanced scalability and effectiveness when dealing with large and complex datasets in particular for approximate arbitrary functions [43]. Therefore, in order to get an overview over the design space this approach based on an initial Halton sequences [44] is a feasible choice. For the surrogate based Optimization (SBO) with the need for local accuracy the state of the art approach with universal Kriging based on the Gaussian kernel is applied here. Kriging is a statistical method with its actual functional form depending on the kernel. It excels in accurately predicting intermediate values, making it ideal for modeling complex, multi-dimensional functions [45]. Kriging is also beneficial for estimating local uncertainty [45]. Both surrogate approaches are based on the **S**urrogate **M**odeling for **A**e**R**o-Data **T**oolbox (*SMARTy*) [46], developed by the DLR.

3 RESULTS

Figure 6 depicts the trend of combined block fuel across the wingspan. It shows trends both with and without load alleviation, and includes an error estimation represented by the standard deviation of the underlying neural network. The figure's lower section also displays the percentage difference in block fuel for both trends relative to their values without load alleviation, highlighting the direct impact of active load alleviation along the wingspan. The trends do not strictly adhere to a single design parameter and are not included in the training data for the surrogate models, except for the reference point. Consequently, further validation of these models is demonstrated through a series of calculated points along both curves, shown in Figure 6. Additionally, the boundary conditions for the case with GMLA are presented.

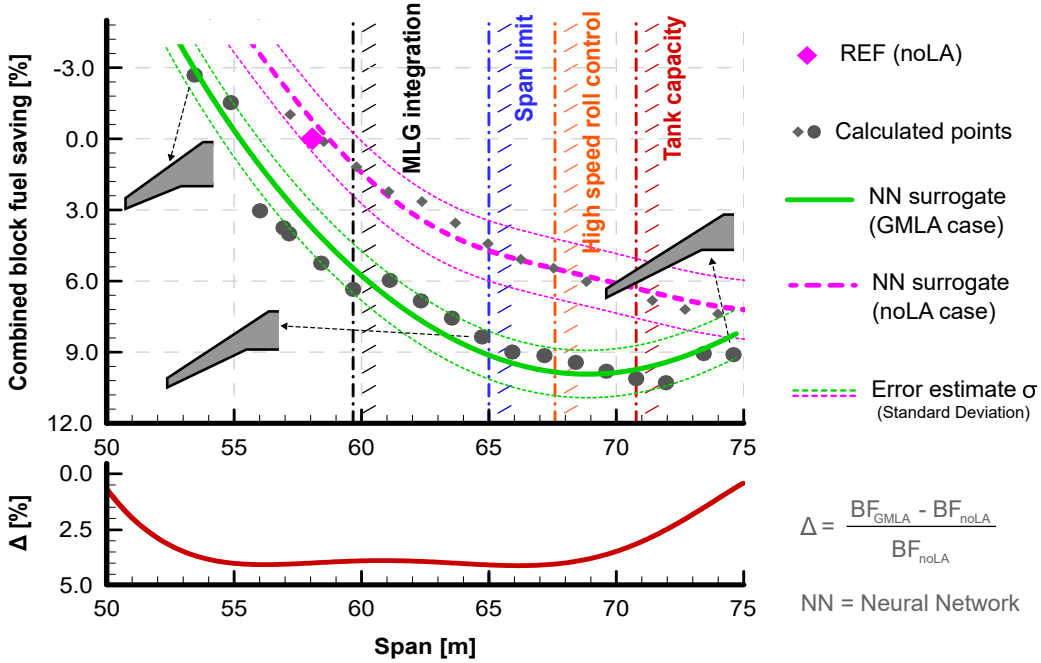

Figure 6: Study results of span variation with and without load alleviation (limits for GMLA case).

Both scenarios show that an increasing wingspan initially enhances the fuel burn efficiency. The slope of these trends decreases, with the GMLA case displaying an early minimum within the observed range. The optimization shown later is therefore expected to enhance the fuel efficiency by at least ten percent. The calculated points align well with the surrogate model predictions, affirming that the standard deviation effectively quantifies the prediction accuracy of the neuronal network. The impact of direct and active load alleviation remains roughly constant at about 4% for wingspans between 55 and 68 meters. Below this range, the effect lessens due to less effective structural load reduction from a shorter lever arm. At larger wingspans, the benefit decreases, indicating that beyond a certain point, aerodynamic gains are constrained by wing flexibility and passive load alleviation becomes more pronounced.

The reference aircraft wing has an aspect ratio of 9.92, a taper ratio of 0.199, a leading edge sweep angle of 32.0 degrees, and a relative span-wise engine position on the wing of 0.34. The relative thickness of the airfoil at the root and kink positions is 0.12. The engine has a bypass ratio of 11.74, providing a sea level static thrust of 330.7 kN. Based on the reference aircraft this study presents three optimized configurations. The first, termed the baseline configuration, maintains a fixed planform while optimizing the local airfoil thickness and twist distribution. The other two configurations extend the optimization to the planform, involving all nine design parameters. One of these is labeled as noLA, indicating no active load alleviation, and the other is identified as GMLA, denoting an optimization with active gust and maneuver load alleviation. Throughout this study, the engine specifications remain unchanged from the reference aircraft. Figure 7 shows the geometrical details of the platform optimizations with and without load alleviation compared to the reference aircraft. Table 3 provides an overview over key data for all discussed configuration.

Table 2: Basic aircraft data of specific configurations.

Configuration	$mWing$ [kg]	OEM [kg]	**AR** [-]	**TR** [-]	**Sweep** [°]	**Kink pos.** [-]	**Block Fuel** $[10^{-4}km^{-1}]$
Reference	25318	116138	9.92	0.199	32.0	0.34	2.0431
Baseline	24374	114477	9.92	0.199	32.0	0.34	1.8598
noLA	25997	114869	13.17	0.289	32.93	0.223	1.6703
GMLA	20971	109502	13.6	0.171	32.35	0.242	1.6438

The optimized configuration without load alleviation (noLA) features an aspect ratio of 13.2, a taper ratio of 0.289, a leading edge sweep angle of 32.93 degrees, and a relative spanwise kink position of 0.223. The airfoil thickness at the root position is 10.3% and 14.0% at the kink position. The optimized configuration with active maneuver and gust load alleviation (GMLA) features an aspect ratio of 13.6, a taper ratio of 0.171, a sweep angle of 32.35 degrees, and a relative spanwise kink position of 0.242. The airfoil thickness at the root position is 8.7% and 14.0% at the kink position. The fuel burn efficiency of the noLA configuration in combined relative block fuel is 10.19% higher than for the baseline and 19.2% higher than for the reference configuration. The wing mass, at approximately 26 tons, is significantly heavier than the wings of these comparative configurations. Nevertheless, the operational empty weight (OEM) is about

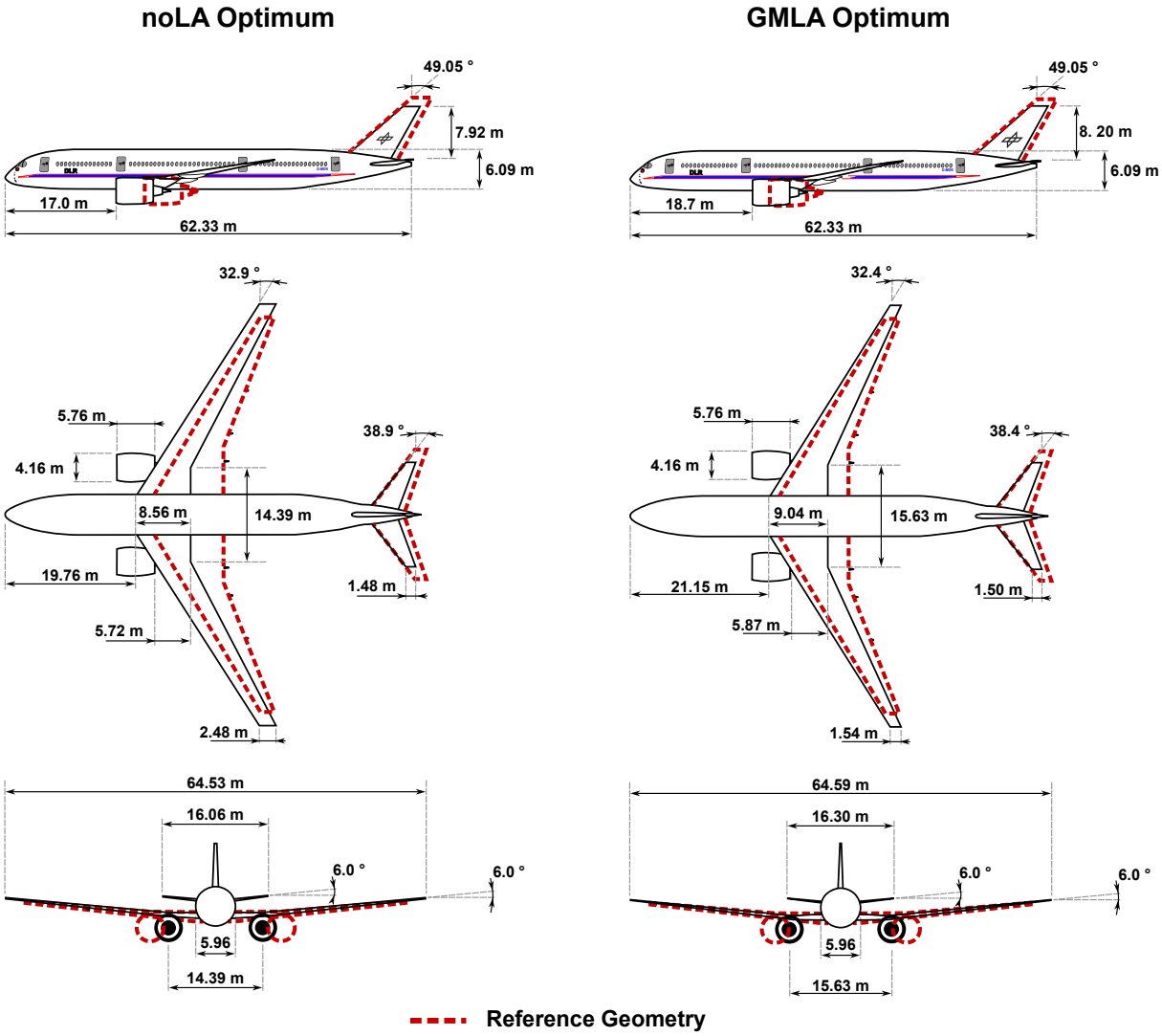

Figure 7: Geometrical details of the noLA and GMLA optimized aircraft compared to the reference.

114.9 tons, similar to the baseline configuration. The maximum takeoff weight is around 205.6 tons. The fuel burn efficiency of the GMLA configuration in combined relative block fuel is 11.61% higher than for the baseline and 20.3% higher than for the reference configuration. The wing mass, at approximately 21 tons, is significantly less than the wing mass of these comparative configurations. The operational empty weight (OEM) is about 109.5 tons. The maximum takeoff weight is around 199.4 tons. Globally, the two optima, with and without load alleviation, differ by about 1.6% in fuel efficiency. Relative to the baseline, the values are 11.6% for the configuration with active load alleviation and 10.19% for the configuration without it.

The presence of load alleviation leads to a wing-driven optimum more pronounced than in scenarios without load alleviation. In the process within this paper, featuring a more detailed wing design, the GMLA case can thus be expected to exhibit a better overall accuracy or

a reduced uncertainty of the overall result compared to the noLA optimum aircraft design. This noLA optimum shows significant performance improvements based on the empennage size reduction, which here is not covered as far in detail as the wing design. The most realistic estimation of the fuel burn potential of load alleviation is a comparison of the baseline and the GMLA configuration and therefore 11.6%. From Figure 6 it can be concluded that regardless of the span the direct effect of load alleviation is around 4% which leaves around 7.6% fuel burn efficiency related to the planform optimization. Figure 8 shows the span-wise lift and local lift coefficient distributions.

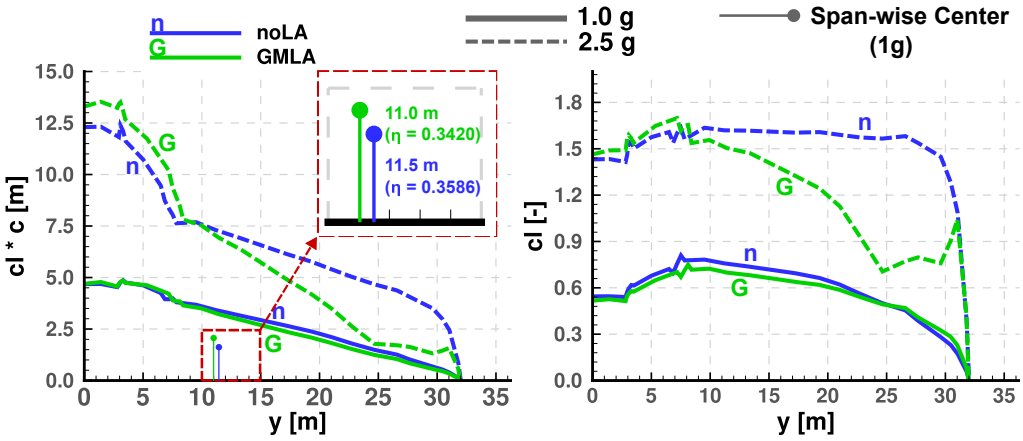

Figure 8: Lift and lift coefficient distribution perpendicular to the beam axis of the noLA compared to the GMLA configuration.

The effect of active load alleviation is evident. Particularly in the outboard wing, this results in a significantly reduced load during the maneuver case. Given the large lever arm of these designs, each with a wingspan of approximately 65 meters, load alleviation has a substantial impact. However, its influence during cruise level flight is minimal, with the differences being almost negligible. The span-wise center of Lift of the noLA optimum lies only 0.5 m further outboard, resulting in a relative position of $\eta = 0.3586$ compared to $\eta = 0.3420$ for the GMLA optimum. This is significantly more inboard than for the aerodynamically beneficial elliptical lift distribution with a span-wise center of $\eta = 0.4244$. This clearly illustrates that active load alleviation, primarily reduces the adverse structural influence of a higher wing span.

4 CONCLUSIONS AND OUTLOOK

This research focused on conceptual aircraft design of a classic tube-and-wing configuration and an evaluation of load alleviation technologies. A software framework was developed, integrating tools from aerodynamics, structural mechanics, and flight control. Through surrogate model-based optimization, the study identified optimal configurations with and without load alleviation. The most realistic estimation of the fuel burn potential from active load alleviation is 11.6%, attributed to both, active load control and concurrent wing planform optimization. Future research should expand the range of considered load cases and investigate flutter constraints. Extending the design scope towards a detailed consideration of the fuselage and empennage could provide a more comprehensive understanding of active load alleviation effects.

Acknowledgements

The presented work is partially co-funded by the Federal Ministry for Economic Affairs and Climate Action (BMWK) as part of the LuFo VI-1 project INTELWI, funding reference: 20A1903L. I would like to thank Prof. Dr. Mark Drela for providing the ASWING license to our aircraft design group.

References

[1] OurWorldinData. *Global airline passenger capacity and traffic*. Source: International Civil Aviation Organization via Airlines for America (2023). Apr. 2023. URL: https://ourworldindata.org/grapher/airline-capacity-and-traffic (visited on 08/29/2023).

[2] David S. Lee et al. "The contribution of global aviation to anthropogenic climate forcing for 2000 to 2018". In: *Atmospheric Environment* 244 (2021), p. 117834. DOI: 10.1016/j.atmosenv.2020.117834.

[3] Constanze Fetting. "The European green deal". In: *ESDN report* 53 (2020).

[4] Europäische Kommission et al. *Flightpath 2050 : Europe's vision for aviation : maintaining global leadership and serving society's needs*. Publications Office, 2011. DOI: doi/10.2777/50266.

[5] Axel Krein and Gareth Williams. "Flightpath 2050: Europe's vision for aeronautics". In: *Innovation for Sustainable Aviation in a Global Environment: Proceedings of the Sixth European Aeronautics Days, Madrid* 30 (2012). DOI: 10.3233/978-1-61499-063-5-63.

[6] Deutsches Zentrum für Luft- und Raumfahrt - DLR e.V. *AUF DEM WEG ZU EINER EMISSIONSFREIEN LUFTFAHRT - Luftfahrtstrategie des DLR zum European Green Deal*. Deutsches Zentrum für Luft- und Raumfahrt e. V. (DLR), 2021. URL: DLR.de/luftfahrtstrategie.

[7] William Richard Graham et al. "The potential of future aircraft technology for noise and pollutant emissions reduction". In: *Transport policy* 34 (2014), pp. 36–51. DOI: 10.1016/j.tranpol.2014.02.017.

[8] Craig L. Nickol. "Technologies and concepts for reducing the fuel burn of subsonic transport aircraft". In: *NATO AVT-209 Workshop on Energy Efficient Technologies*. NF1676L-15121. 2012. URL: https://ntrs.nasa.gov/citations/20120016006.

[9] NASA Aeronautics. "NASA Aeronautics Strategic Implementation Plan: 2019 Update". In: *National Aeronautics and Space Administration (NASA), Whasington, DC, USA* (2023). Tech. Rep. NP-2023-02-3099-HQ
. URL: https://www.nasa.gov/aeroresearch/strategy.

[10] Brian M. Yutko et al. "Conceptual design of a D8 commercial aircraft". In: *17th AIAA Aviation Technology, Integration, and Operations Conference*. 2017, p. 3590. DOI: 10.2514/6.2017-3590.

[11] International Air Transport Association (IATA). *Aircraft Technology Net Zero Roadmap*. Aircraft Technology Net Zero Roadmap, 2023. URL: https://www.iata.org/en/programs/environment/roadmaps/ (visited on 08/28/2023).

[12] Thomas Klimmek et al. "Development of a Short Medium Range Aircraft Configuration for Aeroelastic Investigations using cpacs-MONA". In: (2022). URL: https://elib.dlr.de/194675/.

[13] Johannes Hartmann and Björn Nagel. "Eliminating Climate Impact From Aviation-A system level approach as applied in the framework of the DLR-internal project EXACT". In: *DLRK 2021* (2021). URL: https://elib.dlr.de/148552/.

[14] Ian A. Clark et al. "Aircraft system noise of the NASA D8 subsonic transport concept". In: *Journal of Aircraft* 58.5 (2021), pp. 1106–1120. DOI: 10.2514/1.C036259.

[15] Mark Drela. "Development of the D8 transport configuration". In: *29th AIAA Applied Aerodynamics Conference*. 2011, p. 3970. DOI: 10.2514/6.2011-3970.

[16] Marty K. Bradley et al. *Subsonic ultra green aircraft research. Phase II – Volume I – Truss Braced Wing Design Exploration*. Tech. rep. NASA/CR–2015-218704/Volume I. 2015. URL: https://ntrs.nasa.gov/citations/20150017036.

[17] Edward M Greitzer et al. *N+ 3 aircraft concept designs and trade studies*. Tech. rep. NASA/CR—2010-216794/VOL2. 2010. URL: https://ntrs.nasa.gov/citations/20100042398.

[18] Claire O'Shea. *Next generation experimental aircraft becomes NASA's newest X-Plane*. June 2023. URL: https://www.nasa.gov/press-release/next-generation-experimental-aircraft-becomes-nasa-s-newest-x-plane (visited on 08/28/2023).

[19] Suparnamaaya Prasad et al. "Characterization of atmospheric turbulence as a function of altitude". In: *9th AIAA Atmospheric and Space Environments Conference*. 2017, p. 3064. DOI: 10.2514/6.2017-3064.

[20] Thomas E. Noll et al. "Impact of active controls technology on structural integrity". In: *Journal of Aircraft* 30.6 (1993), pp. 985–992. DOI: 10.2514/3.46443.

[21] Vega Handojo et al. "Potential Estimation of Load Alleviation and Future Technologies in Reducing Aircraft Structural Mass". In: *Aerospace* 9.8 (2022), p. 412. DOI: 10.3390/aerospace9080412.

[22] Simon Binder et al. "The interaction between active aeroelastic control and structural tailoring in aeroservoelastic wing design". In: *Aerospace Science and Technology* 110 (2021), p. 106516. DOI: 10.1016/j.ast.2021.106516.

[23] Simon Thel et al. "A passive load alleviation aircraft wing: topology optimization for maximizing nonlinear bending–torsion coupling". In: *Structural and Multidisciplinary Optimization* 65.5 (2022), pp. 1–17. DOI: 10.1007/s00158-022-03248-3.

[24] Rhea P. Liem et al. "Multimission aircraft fuel-burn minimization via multipoint aerostructural optimization". In: *AIAA Journal* 53.1 (2015), pp. 104–122. DOI: 10.2514/1.J052940.

[25] Sergio Ricci et al. "Aeroelastic Optimization of High Aspect Ratio Wings for Environmentally Friendly Aircraft". In: *AIAA Scitech 2022 Forum*. 2022, p. 0166. DOI: 10.2514/6.2022-0166.

[26] Tobias F. Wunderlich et al. "Global Aerostructural Design Optimization of More Flexible Wings for Commercial Aircraft". In: *Journal of Aircraft* 58.6 (2021), pp. 1254–1271. DOI: 10.2514/1.C036301.

[27] Jia Xu and Ilan Kroo. "Aircraft design with active load alleviation and natural laminar flow". In: *Journal of Aircraft* 51.5 (2014), pp. 1532–1545. DOI: 10.2514/1.C032402.

[28] Markus D. Krengel and Martin Hepperle. "Gust and Maneuver Load Alleviation in Conceptual Overall Aircraft Design". In: *AIAA AVIATION 2023 Forum*. 2023, p. 3369. DOI: 10.2514/6.2023-3369.

[29] Markus D. Krengel and Martin Hepperle. "Potential und Grenzen bei der Optimierung des Flügelgrundrisses mit und ohne Lastabminderung im Flugzeugkonzeptentwurf". In: *DLRK 2023, Stuttgart*. 2023. DOI: 10.25967/610118. URL: https://publikationen.dglr.de/?tx_dglrpublications_pi1%5bdocument_id%5d=610118.

[30] Sebastian Woehler et al. "Preliminary aircraft design within a multidisciplinary and multifidelity design environment". In: 3AF Association Aéronautique et Astronautique de France, 2020. URL: https://elib.dlr.de/185515/.

[31] Mark Drela. "ASWING 5.99 Technical Description—Steady Formulation". In: *Massachusetts Inst. of Technology, Cambridge, MA* (2015).

[32] Mark Drela. "ASWING 5.99 Technical Description–Unsteady Extension". In: *Massachusetts Inst. of Technology, Cambridge, MA* (2015).

[33] Marko Alder et al. "Recent advances in establishing a common language for aircraft design with CPACS". In: *Aerospace Europe Conference 2020, Bordeaux, Frankreich*. 3AF Association Aéronautique et Astronautique de France, 2020. URL: https://elib.dlr.de/134341/.

[34] David Benko et al. "A fresh look at Cauchy's Convergence Criterion". In: *Carpathian Journal of Mathematics* 37.1 (2021), pp. 35–43. URL: https://www.jstor.org/stable/27082080.

[35] Egbert Torenbeek. *Synthesis of subsonic airplane design: an introduction to the preliminary design of subsonic general aviation and transport aircraft, with emphasis on layout, aerodynamic design, propulsion and performance*. Springer Science & Business Media, 2013. 624 pp. ISBN: 978-9048182732.

[36] William H. Mason. "Transonic Aerodynamics of airfoils and wings". In: *Notes in Configuration Aerodynamics, Virginia Tech* 4.4 (2006). URL: https://archive.aoe.vt.edu/mason/Mason_f/ConfigAero.html.

[37] Ed Obert. *Aerodynamic Design of Transport Aircraft*. IOS press, 2009. ISBN: B01JQ6GN86.

[38] Hermann Glauert. *Theoretical relationship for an airfoil with hinged flap. ARC Rep. u.* ARC Rep. Mem. 1095, 1927.

[39] European Aviation Safety Agency. *Certification Specifications and Acceptable Means of Compliance for Large Aeroplanes CS-25*. 2019.

[40] Eytan Adler and Joaquim R.R.A. Martins. "Aerostructural wing design optimization considering full mission analysis". In: *AIAA SCITECH 2022 Forum*. 2022, p. 0382. DOI: 10.2514/6.2022-0382.

[41] Tom Cooper et al. "Global fleet & MRO market forecast commentary". In: *Olyver Wyman* (2018).

[42] Andreas Zell. *Simulation neuronaler netze*. Vol. 1. 5.3. Addison-Wesley Bonn, 1994. 236 pp. ISBN: 978-3322832009. DOI: 10.1007/978-3-322-83200-9.

[43] Kurt Hornik. "Approximation capabilities of multilayer feedforward networks". In: *Neural networks* 4.2 (1991), pp. 251–257. DOI: 10.1016/0893-6080(91)90009-T.

[44] John H. Halton. "On the efficiency of certain quasi-random sequences of points in evaluating multi-dimensional integrals". In: *Numerische Mathematik* 2.1 (1960), pp. 84–90. DOI: 10.1007/BF01386213.

[45] Alexander Forrester et al. *Engineering design via surrogate modelling: a practical guide*. John Wiley & Sons, Ltd, 2008. 240 pp. ISBN: 978-0470770801. DOI: https://doi.org/10.1002/9780470770801.ch2.

[46] Philipp Bekemeyer et al. "Data-Driven Aerodynamic Modeling Using the DLR SMARTy Toolbox". In: *AIAA AVIATION 2022 Forum*. AIAA 2022-3899. DOI: 10.2514/6.2022-3899. URL: https://arc.aiaa.org/doi/abs/10.2514/6.2022-3899.